Organic & Biomolecular Chemistry

ROYAL SOCIETY OF CHEMISTRY

PAPER

View Article Online
View Journal | View Issue

Cite this: *Org. Biomol. Chem.*, 2022, **20**, 1073

On the mechanism of the dyotropic expansion of hydrindanes into decalins†

Hugo Santalla,*[a,b] Olalla Nieto Faza,[a,b] Generosa Gómez,[a,b] Yagamare Fall[a,b] and Carlos Silva López*[a,b]

Received 2nd November 2021,
Accepted 7th January 2022

DOI: 10.1039/d1ob02150h

rsc.li/obc

A combined computational/experimental approach has revealed key mechanistic aspects in a recently reported dyotropic expansion of hydrindanes into decalins. While computer simulations had already anticipated the need for acid catalysis for making this reaction feasible under the mild conditions used in the laboratory, this work places the dyotropic step not into the reaction flask but at a later step, during the work up instead. With this information in hand the reaction has been optimized by exploring the performance of different activating agents and shown to be versatile, particularly in steroid related chemistry due to the two scaffolds that this reaction connects. Finally, the scope of the reaction has been significantly broadened by showing that this protocol can also operate in the absence of the fused six-member ring.

Introduction

In the last decade the combination of computational mechanistic studies and experimental chemistry has yielded excellent dividends in the discovery and development of new transformations.[1] The field of pericyclic reactions is probably the most fertile in results from such a synergistic approach, since (a) the absence of intermediates somehow limits the experimental toolset available for the exploration of their mechanism and (b) computational methods have proved rather accurate when applied to this particular subset of organic reactions.[2] In this regard, computational chemistry has been successful not only in describing in detail the nature of concerted transition states, their aromaticity and orbital symmetry conservation, but also in assessing issues like selectivity, kinetics, *etc*. It is in this field that we have recently explored an unconventional dyotropic[3] ring expansion process that converts hydrindanes into decalins, as represented in Scheme 1.[4]

We initially applied this rearrangement in the field of vitamin D research, but soon after our report, other authors found interesting applications for it. For instance, Sarpong used it to build the complex polycyclic scaffold of diterpene alkaloids belonging to the diconitine family.[5] Similarly, Houk and Feringa reported a closely related mechanism in the ring contraction of bromocycloheptenes. In this case, the dyotropic mechanism is also found to be responsible for the stereospecificity of the contraction.[6] In our original work, we concluded that the migrating sulfonate group had to be protonated in order to lower the high activation barrier associated to the migration process, which would prevent this reaction from occurring at the operating temperatures, otherwise (Scheme 1). However, this claim was only supported by computational simulations, with no experimental evidence found at that time. This fact, together with the high potential of this transformation in synthesis, prompted us to explore its mechanism in greater depth.

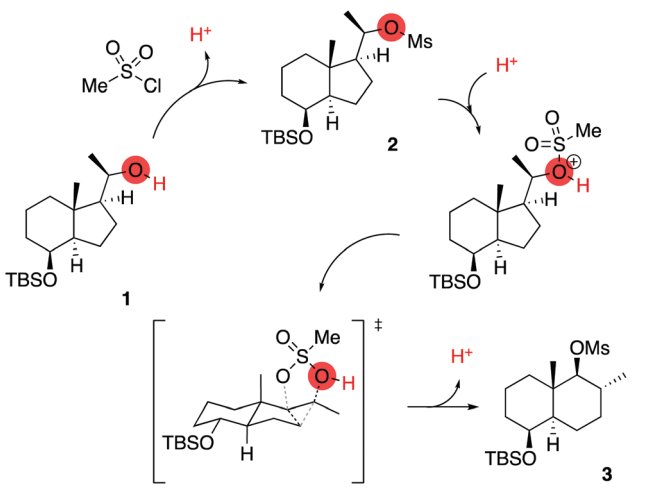

Scheme 1 Proposed mechanism for the hydrindane to decalin ring expansion through a protonated intermediate.

[a]*Departamento de Química Orgánica and Instituto de Investigación Sanitaria Galicia Sur (IISGS), Campus Lagoas-Marcosende, 36310 Vigo, Spain.*
E-mail: hsantalla@uvigo.es, carlos.silva@uvigo.es
[b]*Departamento de Química Orgánica, Campus Lagoas-Marcosende, 36310 Vigo, Spain*

†Electronic supplementary information (ESI) available. CCDC 1998282, 2097540 and 2097547. For ESI and crystallographic data in CIF or other electronic format see DOI: 10.1039/d1ob02150h

Results and discussion

After thorough experimental and computational investigation of this mechanism, we have now obtained solid evidence that confirms that the reaction needs acidic media for the dyotropic migration to happen. Furthermore, this new evidence places the dyotropic step out of the reaction flask and into the chromatography column. This knowledge has been applied to the improvement of reaction conditions and the expansion of the scope of the reaction using it in the construction of a number of different systems.

First, after having run the reaction as described in our previous report, in an attempt to unveil the sought after acidic activator, we analyzed the reaction crude in high detail, using NMR spectroscopy. The results were surprising, since we could not find any signal associated to the presence of mesylate **3**, assigning just the signals belonging to **2**, which corresponds to mesylation of alcohol **1**. This suggests that the ring expansion may be occurring later, perhaps during the work up and, likely, in the separation step. For this reason, we prepared a second experiment in which, to a flask with the reaction crude of the mesylation step, silica was added and stirred for 2 h. Gratifyingly, under these conditions, signals of mesylate **3** were observed in the NMR spectra, confirming that the expansion was completed. In fact, a third experiment proved that reduced reaction times of only 5 minutes or even less for this step are sufficient to promote the dyotropic rearrangement (Scheme 2). These experiments unequivocally confirm that acid is needed for the dyotropic rearrangement to proceed at the working temperatures, as our calculations had predicted. They also unveiled the proton source, which is attributed to the silica used in the purification step, and not the hydroxyl proton in the reaction flask as previously suggested.

Once a complete description of the mechanism was obtained, we attempted to improve yields, increase the versatility of this transformation and, perhaps, obtain further mechanistic details on the dyotropic ring expansion by replacing mesyl chloride with different reagents (Table 1).

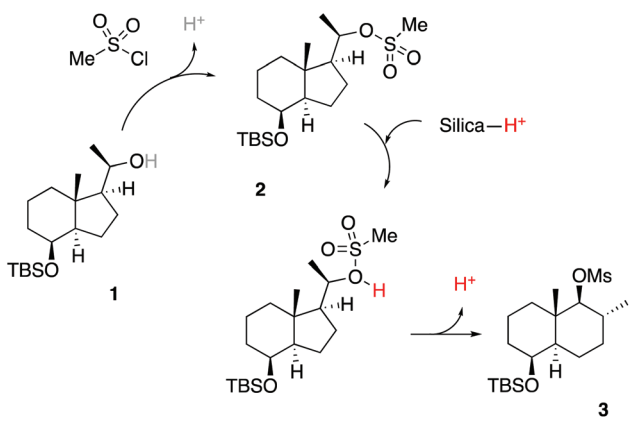

Scheme 2 Mechanism through a protonated intermediate.

Table 1 Series of experiments with different alcohol activating agents to promote the hydrindane **1** ring expansion

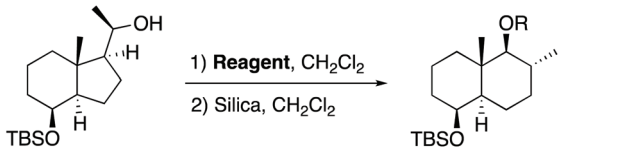

	Reagent	*T*	Product	Yield
1	TsCl, py	0 °C	Decalin 4	83%
2	Ac_2O, py	0 °C	Hydridane 5	25%
3	Naphthyl-SO_2Cl, py	r.t.	Decalin 6	70%
4	$(C_6F_5)SO_2Cl$, Et_3N	r.t.	Hydridane 7	35%
5	*p*-(PhCN)SO_2Cl, Et_3N	0 °C	—	—
6	Tol-CH_2SO_2Cl, Et_3N	0 °C	—	—
7	Tf_2O, Et_3N	−78 °C	Hydridane 8	25%
8	$CySO_2Cl$, Et_3N	r.t.	—	—
9	(PMB)SO_2Cl, Et_3N	0 °C	—	

This exploratory work showcased that not all alcohol activating agents are useful in this transformation. On the one hand, some are unable to effectively activate the secondary alcohol, and the unreacted starting material is recovered (Table 1, entries 5, 6, 8 and 9). All alkylsulfonyl derivatives seem to fall into this category. On the other hand, hydrindanyl sulfonates **5**, **7** and **8** were obtained as a mixture of epimers in low yields (25–35%) when subjected to the activation–expansion protocol (entries 2, 4 and 7, respectively). In these cases, extending the reaction times under silica in CH_2Cl_2 for 2 days did not improve the overall results. It is interesting that in these cases the observed epimerization at the carbynol center takes place during the initial activation step and it occurs in a larger extent the stronger the activating agent employed (for instance, the epimerization ratio with Ac_2O, TfO_2 and $(C_6F_5)SO_2Cl$ is 95 : 5, 84 : 16, 47 : 53, respectively).

According to our previous mechanistic exploration,[4] the solvolysis of the hydrindane and formation of a secondary carbocation would unleash a rearragement cascade in which a decaline would only be a transient structure that is further transformed into a *cys*-decahydroazulene scaffold. This was also consistent with prior experimental evidence registered in the field of pseudoguaianolide sequiterpenes.[7] This accumulated evidence suggests that strong alcohol activating agents may produce fleeting ionic pairs that recombine in a time frame where epimerization is competitive but ring expansion is not. Satisfyingly however, two of the surveyed activating agents yielded the sought after decalins **4** and **6** in good yield (entries 1 and 3). Both could be crystallized and their structure subsequently confirmed by single-crystal X-ray diffraction (Fig. 1).[8,9]

These results suggest that the use of sulfonyl reagents with powerful electron withdrawing groups allow for the activation of the alcohol in the initial hydrindane but the ring expansion step does not take place. Conversely, the use of sulfonyl reagents with electron donating groups thwarts the initial step and the alcohol is not activated, thus resulting in the recovery of the starting material in all cases (Scheme 3). It therefore

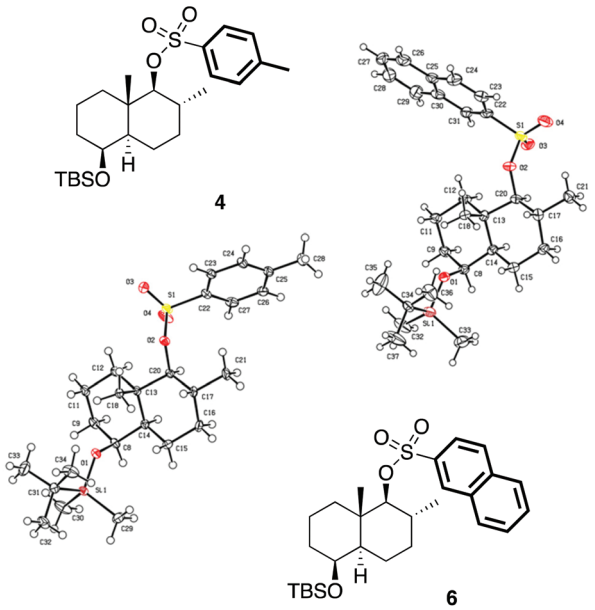

Fig. 1 X-ray structures of new decalins obtained through a dyotropic ring expansion.

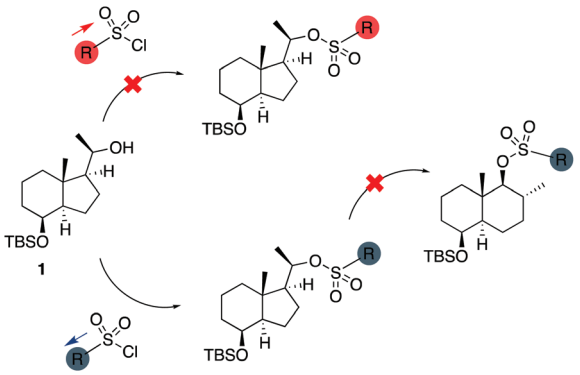

Scheme 3 Influence of substituents in the dyotropic expansion reaction.

seems that a subtle balance between donating and withdrawing effects is key for ensuring that both reaction steps are favourable and achieving the complete transformation of the bicyclic structure from hydrindane to decalin.

It is worth noting that the use of tosyl chloride (entry 1) improved on the originally reported dyotropic expansion, yielding the desired decalin in 83% yield. The toluene fragment seems to provide a sweet spot in the mentioned balance between electron withdrawing and electron donating properties of the activating agent. 2-Naphtalensulfonyl chloride, when reacted with alcohol **1**, also afforded the corresponding hydrindane **9** which was then slowly converted into decalin **6** in low yields (entry 3). In this case, however, allowing for longer reaction times was key to obtain the desired product in synthetically useful yields (70%) (Scheme 4).

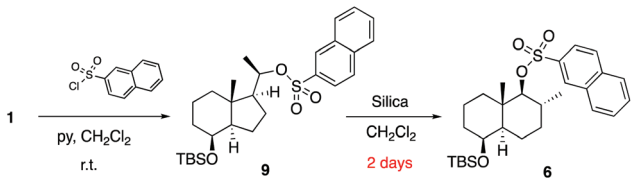

Scheme 4 Slower transformation with naphthyl group.

Regarding the role of silicagel in these dytropic transformation we carried out the reaction using three different heterogeneous activators: Silica Gel 40–63 μm (VWR Chemicals), SilicaFlash® P60 40–63 μm (Silicycle) and Silica Gel beads 2–5 mm (VWR Chemicals). The two gels with smaller particle size activated the concerted migration and produced comparable results in terms of reaction times and yields, whereas the 2–5 mm beads did not produce the expanded product.

To further assess the impact of modifying the acid–base character of the silicagel being used in the work-up process we run a series of experiments oriented towards this end. Alcohol **1** was mesylated and then the migration active product was processed with silica under different conditions (see Table 2).

Attempts to activate the dyotropic expansion by strong Brønsted acids, like *p*-TsOH were unsuccessful, at substoichiometric levels and even with stoichiometric amounts of acid (entries 1–4). Silicagel was inactivated when washed with a weak base, such as Et_3N (entry 5) but kept its catalytic abilities when pre-washed with mild or strong acids, like HFIP or *p*-TsOH (entries 6 and 7). Treatment with a 10% solution of HCl acid also proved unsuccessful to promote the ring expansion, as well as the control experiment (entries 8 and 9). With this information at hand, it seems clear that the intrinsic multicentric and heterogeneous acid character of silicagel is needed for this reaction. Reducing the basicity of silicagel removes its ability to promote the transformation and attempts to replace the heterogeneous acid with homogeneous counterparts also failed.

Computational exploration of the energy profiles for these two new activating agents was also carried out using the same

Table 2 Dyotropic expansion as a function of the work-up procedure

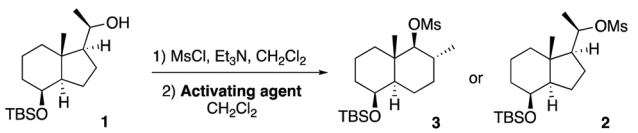

	Activating agent	Product
1	0.1 eq. *p*-TsOH (4 mg, 0.02 mmol)	2
2	0.3 eq. *p*-TsOH (13 mg, 0.06 mmol)	2
3	0.5 eq. *p*-TsOH (21 mg, 0.11 mmol)	2
4	1.0 eq. *p*-TsOH (42 mg, 0.22 mmol)	2
5	Silicagel (washed with Et_3N)	2
6	Silicagel (washed with HFIP)	3
7	Silicagel (washed with *p*-TsOH solution)	3
8	HCl aqueous solution (10%) (2 mL)	2
9	—	2

methodology employed for our seminal work on this chemistry. Density functional theory was used for our simulations.[10,11] Calculations were performed with the dispersion-corrected meta-hybrid density functional ωB97XD[12] and the extended double-ζ quality and polarized def2-SV(P) basis set.[13] Solvation effects were taken into account implicitly *via* the polarizable continuum method (PCM).[14] Optimization under a continuum solvent is possible thanks to the smooth switching function by York and Karplus.[15] All of the calculations were performed with the Gaussian 16 program (further details in the ESI†). Reaction profiles computed in the neutral state (in the absence of a protonating agent) confirmed very high energy demands for the ring expansion process regardless of the nature of the surrounding solvent, although a clear correlation indicates that the process is more favoured the more polar the solvent is (from ~50 kcal mol^{-1} in hexane to ~35 kcal mol^{-1} in *N*-methyl formamide, see Table 2). Contrary to our lack of success in our initial communication, in this occasion we could successfully locate transition states of the protonated substrates and we decided to also study the rearrangement in a range of solvents. In this case, the energy differences among different solvents is narrow (of less than 1 kcal mol^{-1}) and the process is very favourable in all of them, with barriers below 10 kcal mol^{-1} in all cases. Interestingly, a new contradiction with the experimental evidence arises from these simulations. According to experimental observation, the naphthyl derivative activates the rearrangement in a much slower fashion compared to the tosyl fragment. However, in our calculations, the former shows systematically lower barriers than the later (see Table 3). To rationalize this, we hypothesize that the naphthyl fragment, being more hydrophobic and sterically demanding, may obstruct the approach to the silica-gel matrix and hence disfavour the protonation step. The approximations of the solvent environment included in our simulations may certainly not be capturing this effect or other explicit interaction than could potentially reduce the ability of the naphthyl derivative to become protonated through the solvent/silicagel heterogeneous interface. This inability to accurately reproduce the environmental conditions of the heterogeneous activation affect both our previous calculations found in the initial communication of this chemistry and the calculations included in this work. General trends and qualitative information on how the reaction operates can nevertheless be inferred from them.

Table 3 ωB97XD /def2-SVPP activation energies for the hydrindane to decalin ring expansion (in kcal mol^{-1}) computed for the tosyl and naphthyl activating agents (entries 1 and 3 in Table 1) in hexane, dichloromethane, *N*,*N*-dimethylformamide, water and *N*-methylformamide

	Hexane	DCM	DMF	Water	MF
Reaction in the neutral state					
Tosyl	48.3	41.1	38.1	37.1	37.3
Naphthyl	47.5	39.4	35.5	36.7	36.4
Reaction in the monoprotonated state					
Tosyl	9.1	8.7	8.6	8.5	8.4
Naphthyl	5.3	6.0	7.2	4.7	5.5

An interesting question that can be readily addressed, at least at an exploratory level, *via* computation, is whether the full hydrindane core is needed for the rearrangement to occur. In this regard we computed the activation energies for tosylated cyclopentylmethanol derivative **Me-1′** in dichloromethane in neutral and monoprotonated states, and we obtained activation energies of 42.3 and 10.4 kcal mol^{-1}, respectively. These values are only marginally higher than those obtained for the full hydrindane system (41.1 and 8.7 kcal mol^{-1}, respectively, as shown in Table 3). This data was therefore suggesting that the ring expansion may also occur in a much simpler structural motif, albeit, perhaps at slightly harsher thermal conditions. With this information at hand, we ran experiments exploring the possible ring expansion of cyclopentane derivaties (Scheme 5). Simple cyclopentylmethanol mesylate **2′** did not rearrange at room temperature, and it remained inactive when increasing the temperature at 40 °C. However, this simplified structure implied not only removing the cyclohexane ring, but also using a primary alcohol, instead of a secondary one. Guided by the structure of hydrindane **1** and confident in our computational results we prepared the secondary alcohol **Me-1′**, which was also subjected to the ring expansion protocol. Mesylate **Me-2′** did not rearrange at room temperature but, gratifyingly, it did expand when using slightly harsher thermal conditions (40 °C).

The relevance of the degree substitution at the alcohol site was also explored with the full hydrindane system and we could confirm that a secondary alcohol is necessary to promote the rearrangement (see the ESI†).

This methodology has an enormous value to synthesize other steroid structures featuring four fused 6-member-rings using easily available cholesterol derivatives as starting materials as shown in Fig. 2.

Thus, as a proof of concept, we tried this strategy to expand the steroidal structure of the cholesterol derivative stigmasterol

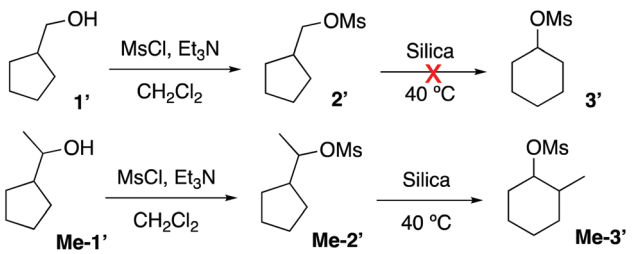

Scheme 5 Expansion proofs with no hydrindane core.

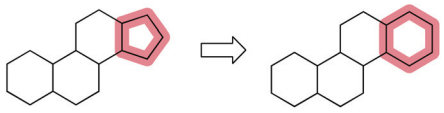

Fig. 2 Synthesis of four 6-member-ring steroids.

through an expedient eight-step process. Six steps are required to prepare the steroid scaffold for the ring expansion (protection of the homoallylic alcohol and instalment of the necessary exocyclic alcohol prior to activating it as a nucleofuge). After the initial six steps we obtained alcohol **15** as depicted in Scheme 6, in an overall 25% yield. This alcohol is ready to be subjected to dyotropic expansion conditions.

Alcohol **15** was therefore converted into mesylate under the conditions outlined in Table 1 (entry 1). Satisfactorily, the ring expanded steroid derivative **16** was formed in 74% yield. As expected, this transformation was carried out in a stereospecific way, thus obtaining only one stereoisomer as shown in Scheme 7.

Next, **16** was deprotected by addition of catalytic amounts of *p*-TsOH over a dioxane/water solution, affording alcohol **17** in 87% yield (Scheme 8).

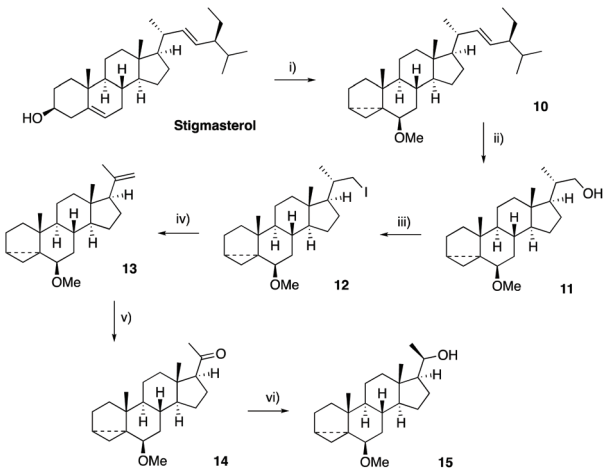

Scheme 6 Obtention alcohol **15** from stigmasterol. Reagents: (i) 1) *p*-TsCl, py, (2) MeOH, py, 75 °C; (ii) O_3, MeOH, CH_2Cl_2, $NaBH_4$; (iii) I_2, PPh_3, Im, THF; (iv) ^{t}BuOK, DMSO, THF, 0 °C; (v) O_3, MeOH, CH_2Cl_2, PPh_3; (vi) L-selectride, THF.

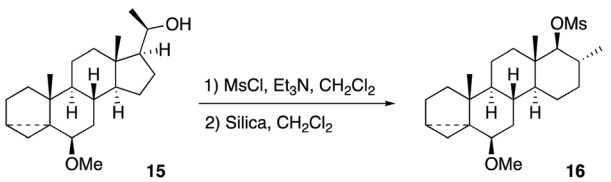

Scheme 7 Dyotropic expansion in steroids.

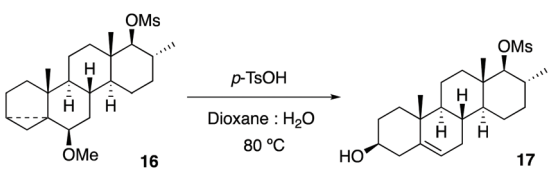

Scheme 8 Deprotection of mesylate **16**.

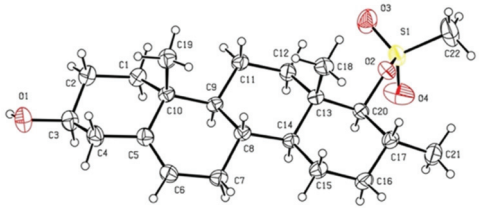

Fig. 3 Structure of alcohol **17** determined by X-ray single-crystal diffraction.

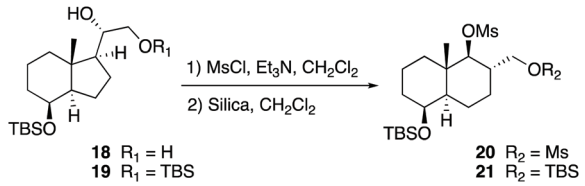

Scheme 9 Dyotropic expansion in functionalized hydrindanes **18** and **19**.

Alcohol **17** is a solid for which a single-crystal was obtained and submitted to X-ray diffraction, achieving an unambiguous proof of the structural data anticipated though NMR experiments (Fig. 3).[16]

To further expand the scope of this rearrangement of hydrindane motifs, we set out to achieve the same transformation on functionalized derivatives that would allow us to access a wider range of structural motifs through further derivatization of the decalin products. Two alternatives were tested, as shown in Scheme 9: first, the dyotropic expansion was carried out on diol **18** under the reaction conditions previously optimized; in a second assay, the same substrate, in which the primary alcohol is protected (**19**), was tested.

Interestingly, the use of diol **18** did not yield the ring expanded product. The corresponding di-mesylate was obtained in 90% yield, but this di-activated compound failed to undergo the dyotropic expansion when treated with silica. However, when alcohol **19** was used as starting material, the expanded product **21** was obtained in 65% yield. This decalin represents an important advance, since it will be possible to obtain novel derivatives with a new level of structural complexity.

Conclusions

In summary, we present new evidence about the way the dyotropic expansion takes place on a hydrindane core and we have expanded this protocol to significantly simpler scaffolds. The initial proposal suggesting the participation of an acid species to catalyse the process has been confirmed and the acid has been identified. Interestingly this transformation was occurring after the alcohol activation, out of the reaction flask, and into the chromatography column.

Different alcohol activating agents have been surveyed in a two pronged strategy. First we aimed at improving the overall performance of this ring expansion, and second, we intended to gain a better understanding of the influence on the expansion of the electronic properties of the activating agent. As a result, we conclude that a balance between donating and withdrawing effects seems to be key for both reaction steps and to the complete transformation of the bicyclic structure from hydrindane to decalin. For these reasons it seems that tosyl chloride is a sweet spot candidate to initiate the rearrangement. The versatility of this methodology was then explored by successfully applying the ring expansion on steroidal structures and novel functionalized hydrindane derivatives.

Conflicts of interest

The authors declare no competing financial interest.

Acknowledgements

This work was supported financially by the Xunta de Galicia (ED431C2017/70). The work of the NMR, MS and Unidade DRX Monocristal divisions of the research support services of the University of Vigo (CACTI) is also gratefully acknowledged. CESGA is acknowledged for generous allocation of HPC time.

Notes and references

1 (*a*) Computation sparks chemical Discovery, *Nat. Commun.*, 2020, **11**, 4811; (*b*) O. Engkvist, P.-O. Norrby, N. Selmi, Y.-h. Lam, Z. Peng, E. C. Sherer, W. Amberg, T. Erhard and L. A. Smyth, Computational prediction of chemical reactions: current status and outlook, *Drug Discovery Today*, 2018, **23**, 1203–1218; (*c*) D. J. Tantillo, Faster, Catalyst! React! React! Exploiting Computational Chemistry for Catalyst Development and Design, *Acc. Chem. Res.*, 2016, **49**, 1079; (*d*) W. T. Borden, Current Applications of Computational Chemistry in JACS—Molecules, Mechanisms, and Materials, *J. Am. Chem. Soc.*, 2011, **133**, 14841–14843.

2 (*a*) K. N. Houk, F. Liu, Z. Yang and J. I. Seeman, Evolution of the Diels–Alder Reaction Mechanism since the 1930s: Woodward, Houk with Woodward, and the Influence of Computational Chemistry on Understanding Cycloadditions, *Angew. Chem., Int. Ed.*, 2020, **60**, 12660–12681; (*b*) D. Birney, Theory, Experiment and Unusual Features of Potential Energy Surfaces of Pericyclic and Pseudopericyclic Reactions with Sequential Transition Structures, *Curr. Org. Chem.*, 2010, **14**, 1658–1668; (*c*) J. B. Siegel, A. Zanghellini, H. M. Lovick, G. Kiss, A. R. Lambert, J. L. St Clair, J. L. Gallaher, D. Hilvert, M. H. Gelb, B. L. Stoddard, K. N. Houk, F. E. Michael and D. Baker, Computational design of an enzyme catalyst for a stereoselective bimolecular Diels-Alder reaction, *Science*, 2010, **329**, 309–313; (*d*) C. Silva López, O. Nieto Faza and Á. R. de Lera, Computational Study and Analysis of the Kinetic Isotope Effects of the Rearrangement of cis-Bicyclo [4.2.0]oct-7-ene to cis,cis-Cycloocta-1,3-diene, *Org. Lett.*, 2006, **8**, 2055–2058; (*e*) X.-N. Wang, E. H. Krenske, R. C. Johnston, K. N. Houk and R. P. Hsung, Torquoselective Ring Opening of Fused Cyclobutenamides: Evidence for a Cis,Trans-Cyclooctadienone Intermediate, *J. Am. Chem. Soc.*, 2014, **136**, 9802–9805.

3 (*a*) M. T. Reetz, Dyotropic Rearrangements, a New Class of Orbital-Symmetry Controlled Reactions. Type I, *Angew. Chem., Int. Ed. Engl.*, 1972, **11**, 129–130; (*b*) M. T. Reetz, Dyotropic Rearrangements, a New Class of Orbital-Symmetry Controlled Reactions. Type II, *Angew. Chem., Int. Ed. Engl.*, 1972, **11**, 131–132; (*c*) I. Fernández, M. A. Sierra and F. P. Cossío, Stereoelectronic Effects on Type I 1,2-Dyotropic Rearrangements in Vicinal Dibromides, *Chem. – Eur. J.*, 2006, **12**, 6323; (*d*) I. Fernández, F. M. Bickelhaupt and F. P. Cossío, Type-I Dyotropic Reactions: Understanding Trends in Barriers, *Chem. – Eur. J.*, 2012, **18**, 12395; (*e*) I. Fernández, F. P. Cossío and M. A. Sierra, Dyotropic Reactions: Mechanisms and Synthetic Applications, *Chem. Rev.*, 2009, **109**, 6687–6711; (*f*) R. L. Davis and D. J. Tantillo, Dissecting a Dyotropic Rearrangement, *J. Org. Chem.*, 2010, **75**, 1693–1700; (*g*) R. L. Davis, C. A. Leverett, D. Romo and D. J. Tantillo, Switching Between Concerted and Stepwise Mechanisms for Dyotropic Rearrangements of beta-Lactones Leading to Spirocyclic, Bridged gamma-Butyrolactones, *J. Org. Chem.*, 2011, **76**, 7167–7174; (*h*) C. A. Leverett, V. C. Purohit, A. G. Johnson, R. A. Davis, D. J. Tantillo and D. Romo, Dyotropic Rearrangements of Fused Tricyclic-beta-Lactones: Application to the Synthesis of (-)-Curcumanolide A and (-)-Curcumalactone, *J. Am. Chem. Soc.*, 2012, **134**, 13348; (*i*) X. Lei, Y. Li, Y. Lai, S. Hu, C. Qi, G. Wang and Y. Tang, Strain-Driven Dyotropic Rearrangement: A Unified Ring-Expansion Approach to α-Methylene-γ-butyrolactones, *Angew. Chem., Int. Ed.*, 2021, **60**, 4221.

4 H. Santalla, O. Nieto, G. Gómez, Y. Fall and C. Silva, From Hydrindane to Decalin: A Mild Transformation through a Dyotropic Ring Expansion, *Org. Lett.*, 2017, **19**, 3648–3651.

5 K. G. M. Kou, S. Kulyk, C. J. Marth, J. C. Lee, N. A. Doering, B. X. Li, G. M. Gallego, T. P. Lebold and R. Sarpong, A Unifying Synthesis Approach to the C_{18}-, C_{19}-, and C_{20}-Diterpenoid Alkaloids, *J. Am. Chem. Soc.*, 2017, **139**, 13882–13896.

6 S. S. Goh, P. A. Champagne, S. Guduguntla, T. Kikuchi, M. Fujita, K. N. Houk and B. L. Feringa, Desymmetrization of meso-Dibromocycloalkenes through Copper(I)-Catalyzed Asymmetric Allylic Substitution with Organolithium Reagents, *J. Am. Chem. Soc.*, 2018, **140**, 4986–4990.

7 (*a*) J. B. Hendrickson, C. Ganter, D. Dorman, H. Link and V. Sesquiterpenes, The stereospecific synthesis of pseudoguaianolide sesquiterpenes, *Tetrahedron Lett.*, 1968, **9**, 2235; (*b*) C. H. Heathcock, E. G. DelMar and S. L. J. Graham, Synthesis of sesquiterpene antitumor

lactones. 9. The hydronaphthalene route to Pseudoguaianes. Total synthesis of (±)-Confertin, *J. Am. Chem. Soc.*, 1982, **104**, 1907.

8 Crystallographic data have been collected at 100 K using a Bruker D8 Venture diffractometer with a Photon II CMOS detector and Mo-Kα radiation (λ = 0.71073(Å) generated by an Incoatec high brilliance microfocus source equipped with Incoatec Helios multilayer optics. The software APEX3 has been used for collecting frames of data, indexing reflections, and the determination of lattice parameters, SAINT for integration of intensity of reflections, and SADABS for scaling and empirical absorption correction. The structure has been solved by dual-space algorithm using the program SHELXT. All non-hydrogen atoms have been refined with anisotropic thermal parameters by full-matrix least-squares calculations on *F* using the program SHELXT with OLEX2. Hydrogen atoms have been inserted at calculated positions and constrained with isotropic thermal parameters. The sample has crystallized in the chiral space group *P*1. The absolute configuration has been determined by anomalous dispersion effects in diffraction measurements on the crystal [Flack parameter = 0.037(18)]. The asymmetric unit consists of four independent molecules. Drawings were produced with PLATON. The structural data have been deposited with the Cambridge Crystallographic Data Centre (CCDC) with reference number CCDC 2097540.†

9 Hydrogen atoms have been inserted at calculated positions and constrained with isotropic thermal parameters. The sample has crystallized in the chiral space group $P2_1$. The absolute configuration has been determined by anomalous dispersion effects in diffraction measurements on the crystal using Bayesian statistics on Bijvoet differences [*P*2(true) = 1.000, *P*3(true) = 1.000, *P*3(rac-twin) = 0.1×10^{-10} and *P*3(false) = 0.3×10^{-51}]. The asymmetric unit consists of two independent molecules; in one molecule, the TBS group is disordered over two positions, the site occupation factors have been refined converging to 63 : 37. Drawings have been produced with PLATON. The structural data have been deposited with the Cambridge Crystallographic Data Centre (CCDC) with reference number CCDC 2097547.†

10 P. Hohenberg and W. Kohn, Inhomogeneous electron gas, *Phys. Rev.*, 1964, **136**, B864.

11 W. Kohn and L. Sham, Self-consistent equations including exchange and correlation effects, *Phys. Rev.*, 1965, **140**, A1133.

12 J. D. Chai and M. Head-Gordon, Long-range corrected hybrid density functionals with damped atom–atom dispersion corrections, *Phys. Chem. Chem. Phys.*, 2008, **10**, 6615.

13 F. Weigend and R. Ahlrichs, Balanced basis sets of split valence, triple zeta valence and quadruple zeta valence quality for H to Rn: Design and assessment of accuracy, *Phys. Chem. Chem. Phys.*, 2005, **7**, 3297.

14 J. Tomasi, B. Mennucci and R. Cammi, Quantum mechanical continuum solvation models, *Chem. Rev.*, 2005, **105**, 2999.

15 D. M. York and M. Karplus, Smooth solvation potential based on the conductor-like screening model, *J. Phys. Chem. A*, 1999, **103**, 11060.

16 Hydrogen atoms were inserted at calculated positions and constrained with isotropic thermal parameters except for the hydrogen atoms of the hydroxyl groups, which were located from a Fourier-difference map and refined isotropically. The asymmetric unit consists of two independent molecules. The absolute configuration has been established by anomalous dispersion effects in diffraction measurements on the crystal [Flack parameter = −0.020 (11). Drawings were produced with PLATON. The structural data have been deposited with the Cambridge Crystallographic Data Centre (CCDC) with reference number CCDC 1998282.†